Computer Aided Detection of Prostate Cancer Using T2, DWI and DCE MRI: Methods and Clinical Applications

Henkjan Huisman[1], Pieter Vos, Geert Litjens,
Thomas Hambrock, and Jelle Barentsz

Diagnostic Image Analysis Group, Dept. Radiology
Radboud University Nijmegen Medical Centre,
Nijmegen, The Netherlands
h.huisman@rad.umcn.nl
http://www.diagnijmegen.nl

Abstract. One in 10 men will be diagnosed with prostate cancer during their life. PSA screening in combination with MR is likely to save lifes at low biopsy and overtreatment rates. Computer Aided Diagnosis for prostate MR will become mandatory in a high volume screening application. This paper presents an overview including our recent work in this area. It includes screening MR setup, quantitative imaging features, prostate segmentation, and pattern recognition.

Keywords: computer aided diagnosis, prostate cancer, segmentation, pattern recognition, screening.

1 Introduction

Prostate cancer is the most commonly diagnosed cancer among men and remains the second leading cause of cancer death in men. In 2009, approximately 192,000 in the United States (US) and 9600 in the Netherlands (NL) men were diagnosed with prostate cancer, and 27,000 (US) and 2400 (NL) men died from this disease [20] and (http://www.cbs.nl). The prostate specific antigen (PSA) blood test disseminated 20 years ago, and helped shift the disease stage at the time of diagnosis to a much lower and potentially more curable stage. However, early detection of prostate cancer remains a source of uncertainty and controversy.[20]

Recently, it has been established that PSA and systematic transrectal ultrasound (TRUS) testing can reduce prostate cancer mortality. In a large intention to screen trial, Schroder et al [12] showed a mortality reduction of 20% (improved trial showed 30% [11]). The Schroder clinical workflow had two major problems: low specificity of the PSA test and biopsy as subsequent gold standard. The results showed that 1410 men would need to be screened and 48 cases of prostate cancer need to be treated to prevent one death from prostate cancer.

Magnetic resonance imaging (MRI) can be used to increase specificity, guide biopsy, and improve staging. Prostate MRI has evolved since its first application

A. Madabhushi et al. (Eds.): Prostate Cancer Imaging 2010, LNCS 6367, pp. 4–14, 2010.

in the late 80's [4]. This millennium saw the start of high resolution 3D T2 weighted sequences and 3D dynamic contrast enhanced MR (DCEMR), later followed by 3D diffusion weighted imaging (DWI). Localization of prostate cancer can be performed at a high diagnostic accuracy and has been applied in a first clinical application: MR guided intensity modulated radiotherapy planning [1,7]. Tanimoto et al. [14] using a combination of T2 weighted, DWI, and DCEMR concluded that in patients with a PSA level over 4 ng/ml unnecessary biopsy can be avoided without missing prostate cancer. A recent development is to perform MR guided biopsy of MR determined tumor suspicious regions after having a positive MR. This approach proved to be an accurate method to detect clinically significant prostate cancer in men with repeat negative biopsies and increased PSA levels.[2]

Computer aided diagnostic tools will become essential if mass application of MR would becomes a viable option. Reporting the huge volume of prostate MR accurately and efficient will require skills and the right tools including computerized analysis techniques that help to reduce oversight and interpretation errors. In this paper we describe some of our efforts and recent development on computer aided diagnosis applied to prostate MR.

2 Role of MR in Screening

In the Netherlands 2400 men die each year of prostate cancer. In the population 50-80 yr (2.000.000) that would amount to an incidence of aggressive prostate cancer of about 0.1%, where aggresive is defined as lifethreatening. Similar to breast cancer (same order of incidence), screening by repeat testing can find a substantial number of these 0.1% that require treatment at a stage where cure is still possible. It is essential for screening not to inflict unnescessary harm to men without aggressive cancer, therefore a high specificity of the screening test is essential. In contrast to breast cancer, there is a high incidence of non agressive prostate cancer: most men die with prostate cancer, but not from prostate cancer. These non-aggressive cancers do not require treatment and it is thus important to discriminate agressive from non-agressive cancers.

The PSA test alone is not suitable for screening due to its low specificity. At a PSA threshold of 4 [ng/ml] the sensitivity is 51% at a specificity of 91% for detecting aggressive cancers. At a PSA threshold of 3, the sensitivity is 68% at a specificity of 85% [20]. A PSA level of 3 in a group of 10.000 men with on average 10 aggressive cancers would result in about 7 cancers to be correctly found. The same PSA test however will also be positive for 1500 men. In the current workflow (see figure 1) this would mean 1500 unnescessary biopsies. The biopsy is a second test to find the 7 cancers requiring treatment. Regular systematic first session biopsies have a sensitivity in between 60 to 70%. Moreover, biopsy has only 50 to 70 % accuracy to predict true GS in prostatectomy. It is obvious that aggressive cancers will be missed and over- and undertreatment will result.

We are currently investigating means to reduce the number of unnecessary biopsies and increase the diagnostic yield of the biopsies by using MR as a

second test after PSA testing. Early results show that MR can operate at a sensitivity of 95% with a specificity of 74% [14]. At that setting about 1100 (74% of 1500) unnescessary biopsies can be avoided. Moreover, the MR can guide the biopsy resulting in more representative and fewer cores [2]. The huge reduction in number of biopsies may render prostate MRI cost-effective. Further research should focus on higher specificity MRI and augmenting TRUS to include MR as guidance using automatical, fast and accurate techniques, e.g. [5].

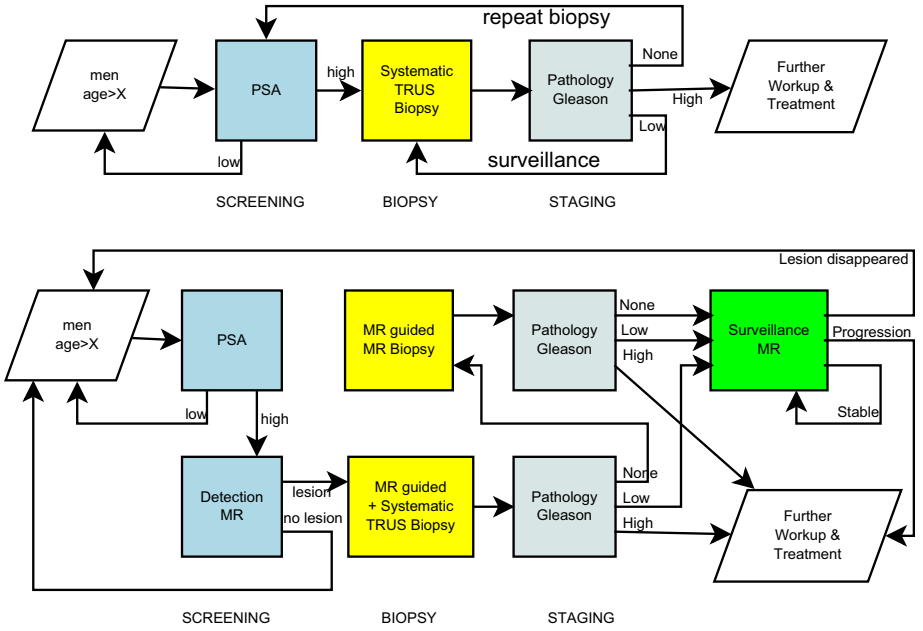

Fig. 1. Prostate cancer detection workflows. Top workflow represents the current situation. The bottom workflow is our proposed future situation including MR.

3 Quantitative Image Features

Diagnostic imaging and computer aided diagnosis require discriminative image features (or biomarkers) that significantly differentiate (aggressive) prostate cancer from other physiological changes. The raw MR sequences often require further processing to reduce for example the coil sensitivity profile or dependencies on administered contrast agent profile. In this section we focus on our recent work on three types of image features: proton relaxation, diffusion weighted imaging and pharmacokinetic DCE-MRI.

3.1 T1 and T2 Relaxation

Quantification of T1 and/or T2 relaxation can be done on the MR machine with dedicated sequences. These sequences are often time consuming, consequently

producing either low resolution or are being too slow for practical use in prostate MR. We have been using the method by Hittmair et al.[3] in dynamic contrast enhanced MR to quantify tracer concentration. It uses an additional proton density weighted MR sequence that adds only a minute to the total acquisition time. The method also produces T1 estimates (or R1=1/T1, see paper appendix). The original method was setup using FLASH sequences assuming a gradient echo signal model. We have extended the method to handle any sequence model. T1 relaxation is a good biomarker to identify recent biopsy locations because hemorrhages resemble malignancy due to the strong and fast contrast enhancement. We use it as one of the features in our CAD systems [18], but we also display T1 images to the clinician.

T2 estimation seemed feasible as well with the above method. As prostate MR includes one or more T2 weighted images. we generalized the Hittmair method further to estimate T2 from a T2 weighted and a proton density sequence and known sequence models [17]. The T2 weighted and the proton density turbo spin echo sequence signals at voxel position x are modelled by:

$$s_{t2w}(x) = G_{t2w} sin(\theta_{t2w}) \rho(x) exp(-TE/T2(x)) \tag{1}$$

$$s_{pd}(x) = G_{pd} sin(\theta_{pd}) \rho(x) \tag{2}$$

where G represents the gain setting and θ the flip angle and ρ is a function comprising proton density fluctuations and coil profile at location x. The $T2$ at position x is then derived by rewriting the above equation to:

$$T2(x) = \frac{-TE}{log(s_{t2w}(x)) - log(s_{pd}(x)) - log(\eta_{t2w,pd})}, \tag{3}$$

where $\eta_{t2w,pd}$ is the gain ratio estimated using a per patient reference fat tissue with know relaxation properties. The additional effort in that work was to also compensate for movement and deformation of the prostate in between the 15 minutes of the two sequences. The estimated T2 was validated by assessing its diagnostic accuracy. The area under the ROC curve for discriminating benign and malignant lesions was 0.64 for the unprocessed T2 weighted images and 0.86 for our T2 estimate. Further validation with additional T2 estimator sequences showed very good correlation (r=0.97).

3.2 Diffusion Weighted Imaging

Diffusion Weighted Imaging (DWI) uses sequences that are sensitive to changes in random Brownian motion properties of water molecules (diffusion) in tissue. The degree of restriction to water diffusion in biologic tissue is inversely correlated to tissue cellularity and the integrity of cell membranes. Quantitative analysis can be made using the apparent diffusion coefficient (ADC) derived from several DWI images at different b strengths. The clinical role of DWI in tumor localization with the prostate has extensively been reported before.

We have established that prostate cancer Gleason Score (GS) is strongly correlated with ADC[2]. We have also established that a normalized ADC value

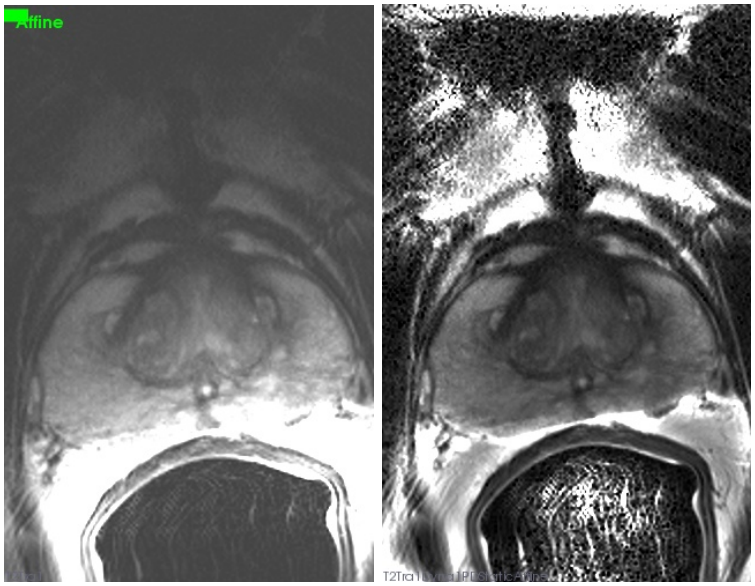

Fig. 2. Example images to demonstrate the effectiveness of the T2 estimation method. To the left a slice from the original T2 weighted images, to the right the T2 estimate of the same slice. The coil profile in the prostate has clearly reduced allowing more narrow window settings and show more contrast. Notice the contrast difference of a hypo dense lesion in the left periferal zone of the prostate (arrow).

(using both surrounding and mirror normal PZ) is even stronger correlated to tumor aggressivity. We hypothesize that either ADC is also dependent on normal prostatic tissue physiology and that normal values vary significantly per patient, or ADC is still dependent on MR machine settings that differ per patient.

3.3 Pharmacokinetic DCEMR

Pharmacokinetic (PK) MR features quantify blood flow, permeability and tissue extracellular volume. The volume transfer constant $K^{trans}[min^{-1}]$ under permeability limited conditions quantifies the permeability surface area of tissue vasculature and is the most diagnostic feature [1]. Various PK estimation methods exist, generally assuming a two compartment tissue model [15]. We have investigated robust and fast DCEMR curve fitting methods [6] and later on extended this to pharmacokinetic modeling [7] integrated with a reference tissue method [9] to estimate the arterial input function (AIF). The AIF drives the tissue model and directly affects the output. We have established that AIF estimation strongly affects the diagnostic accuracy of PK methods [16]. In a CAD application the common population based AIF achieved an AUC of 0.65 whereas the reference tissue method achieved 0.80. In that same publication we presented an automatic method to segment the reference tissue region.

4 Computer Aided Detection

Computer aided detection (CAD) is commonly used in breast cancer screening to help reduce errors in oversight and interpretation. CAD systems generally follow a radiologist perception strategy. Within the organ region a quick scan is performed that results in several initial findings. Each of these findings is further investigated and if any finding is then above a threshold of suspiciousness the person is recalled for further diagnostic work-up. The initial voxel based detector and the lesion classifier are both pattern recognition systems trained on sufficient annotated cases with validated ground truth.

4.1 Prostate Segmentation

Segmentation of the prostate is required to reduce false positives in computer aided detection of malignant lesions. Segmentation is challenging due to the heterogeneity of the zonal anatomy and embedding in variable context. The prostate is situated in between bladder, rectum, two levator ani muscles, fat, neuro vascular bundles, pelvic bone and penis. Single object segmentation strategies that do not account for this heterogeneous context of the prostate (e.g. region growing, deformable surface models) are unlikely to produce satisfactory results. A first context based method was published by Klein et al.[8]. They applied atlas based segmentation on MR to automatically delineate the prostate in a radiotherapy planning application. They showed good results on the majority of cases. However, the population variation was such that the atlas based population model could not segment all the cases robustly. Furthermore, their method was rather computationally expensive, which would be a problem for large scale application.

We propose a new parametric multi-object probabilistic anatomy model based prostate segmentation method that incorporates context using a population model. The pelvic anatomy and modality appearance are modeled by a set of synthetic parametric anatomy objects. Each object has several parameters to define shape and appearance. The complete pelvic model is characterized by a parameter vector x. A population based probability function $p(x)$ is defined that returns the probability of a pelvic model realization to occur in a population. The pelvic model is fitted to the MR images by finding the optimal set of parameters x_{opt} that maximize the appearance correlation and probability in the population. The appearance correlation is computed by simulating pelvic MR images and correlate these with the actual MR images. The population model constrains the pelvic model parameters to feasible solutions within the population. The population model not only constrains individual anatomical objects to be within a certain range (e.g. prostate diameter between 2-6cm), but also captures the contextual relation between objects (rectum is beneath prostate). The optimal pelvic model is then used to segment the images by probabilistic modeling. Each anatomic object defines a spatial and grey value likelihood. For each voxel the likelihood is computed for each anatomical object which is based on position and grey value(s). The segmentation then results by assigning the most likely anatomic object label to each voxel.

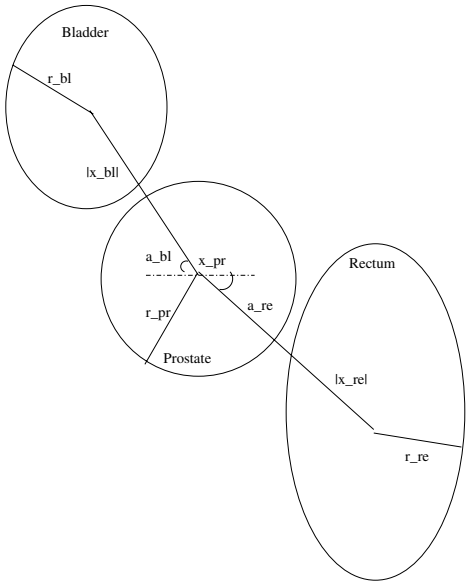

Fig. 3. Parametric pelvic anatomical model definition

Estimating the population model function would require large training databases for even modest pelvic anatomy models. We propose a solution to redefine the anatomy model such that context is captured in several parameters and that these parameters are independent. For example, the prostate and rectum center location stored individually requires 6 parameters, none of which individually captures the distance between the two (context). A redefinition of parameters such that the rectum position is defined by a distance from and angle to the prostate captures context, and also renders the parameters reasonably uncorrelated. We have redefined the above pelvic model parameters to x' (see also Figure 3). Assuming independence the population probability function can be redefined as a multiplication of Gaussians $\mathcal{N}$:

$$p(x') = \prod \mathcal{N}_i \tag{4}$$

Each parameter (i) of the rewritten pelvic model is characterized by a mean and standard deviation. This can be estimated from even a modest training set. Moreover, it allows integration of explicit prior knowledge. For example, prostate size is on forehand known to be within a certain range. Similarly are the grey value distribution of the appearance of several anatomic objects. Figure 4 shows an example segmentation achieved by this method.

4.2 Initial Detector

Our first prototype initial detector [19] used a multi-scale Hessian matrix blob detection filter [10] applied to the ADC map. Peak (local maxima) coordinate

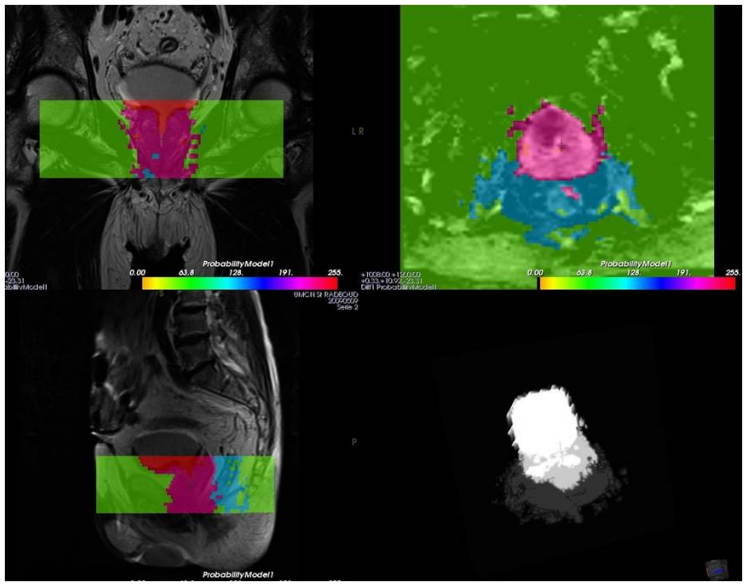

Fig. 4. An example pelvic segmentation using our multi object anatomical model. The pelvic model comprised prostate, rectum, bladder and a other class.

detection within a 5 mm region is performed to localize suspicious findings that serve as input to the lesion characterization stage. In the mean time the data set comprises 216 clinical patients scheduled between January and December 2009 that had elevated PSA levels (mean 14ng/ml range:1-58) and one negative biopsy. Histopathology confirmed the presence of PCa in 43 patients. The detection method currently has a sensitivity of 64% at a 6 false positives per patient.

Currently we are working on a multi-feature detection system, using a voxel based Support Vector Machine classifier in conjunction with a lesion based classifier. Examples of voxel features are DCE MRI based features like Ktrans and ve, diffusion based values like ADC and blobness outputs.

4.3 Lesion Characterization

For lesion characterization we compute several region based features and classify these with a trained SVM classifier. Several region based tumor features exploit the heterogeneity of a malignant lesion. Similar to breast MR hotspot analysis determines the malignancy of a lesion by its most aggressive part. A robust, simple method is to use region quartiles. One of our best features is the 3rd quartile of Ktrans in a region [18]. A potentially improved hot spot analysis method currently researched for application in breast MR is Mean-Shift cluster analysis [13].

In addition we are also developing an automatic suspicious region segmentation system to segment the region. We use a custom cost function in combination

with a LBFGSb optimization method to segment the suspicious region. The cost function is a combination of a population based model and an appearance model.

$$\arg\min_{\boldsymbol{x}} f(x) = p(\boldsymbol{x}) + a(\boldsymbol{x}) \tag{5}$$

Here $p(\boldsymbol{x})$ represents the population model and $a(\boldsymbol{x})$ the appearance model. Also $f(\boldsymbol{x})$ is the complete cost function and $\boldsymbol{x}$ is a set of parameters that is optimized. An example of a parameter that appears in the population model is the radius of the lesion. We assume a normal distribution on the radius, because we know what lesion sizes we can expect in a clinical setting. An example of a parameter in the appearance model can be the mean ADC, because we know that lesions often have a lower ADC value.

After segmentation a number of feature can be extracted from the segmented region, like volume, principle components, mean values and quartiles of quantitative features. These are fed into a trained SVM classifier, after which a probably per region is obtained. This way the false positives we obtain from the voxel classifier can be further reduced.

5 Discussion

Screening using prostate MR can be cost effective in screening due to biopsy reduction. The high volume of imaging requires CAD to assist clinicians in fast and accurate reporting. We developed one of the first fully automatic computer aided detection systems for prostate cancer detection on MR. We have shown good results with quantitative features obtained using robust, automatic and dedicated methods. An automated segmentation method of the prostate has been developed that is robust, fast and sufficiently accurate for application in CAD. We are currently exploring further improvements and setting up observer experiments to validate the CAD methods.

References

1. Fütterer, J.J., Heijmink, S.W.T.P.J., Scheenen, T.W.J., Veltman, J., Huisman, H.J., Vos, P., Hulsbergen-Van de Kaa, C.A., Witjes, J.A., Krabbe, P.F.M., Heerschap, A., Barentsz, J.O.: Prostate cancer localization with dynamic contrast-enhanced MR imaging and proton MR spectroscopic imaging. Radiology 241(2), 449–458 (2006)
2. Hambrock, T., Somford, D.M., Hoeks, C., Bouwense, S.A.W., Huisman, H., Yakar, D., van Oort, I.M., Witjes, J.A., Fütterer, J.J., Barentsz, J.O.: Magnetic resonance imaging guided prostate biopsy in men with repeat negative biopsies and increased prostate specific antigen. J. Urol. 183(2), 520–527 (2010)
3. Hittmair, K., Gomiscek, G., Langenberger, K., Recht, M., Imhof, H., Kramer, J.: Method for the quantitative assessment of contrast agent uptake in dynamic contrast-enhanced MRI. Magn. Reson. Med. 31(5), 567–571 (1994)
4. Hricak, H., Dooms, G.C., McNeal, J.E., Mark, A.S., Marotti, M., Avallone, A., Pelzer, M., Proctor, E.C., Tanagho, E.A.: MR imaging of the prostate gland: normal anatomy. AJR Am. J. Roentgenol. 148(1), 51–58 (1987)

5. Hu, Y., et al.: Mr to ultrasound image registration for guiding prostate biopsy and interventions. Med. Image Comput. Comput. Assist. Interv. 12(Pt 1), 787–794 (2009)
6. Huisman, H.J., Engelbrecht, M.R., Barentsz, J.O.: Accurate estimation of pharmacokinetic contrast-enhanced dynamic MRI parameters of the prostate. Journal of Magnetic Resonance Imaging 13(4), 607–614 (2001)
7. Huisman, H.J., Fütterer, J.J., van Lin, E.N.J.T., Welmers, A., Scheenen, T.W.J., van Dalen, J.A., Visser, A.G., Witjes, J.A., Barentsz, J.O.: Prostate cancer: precision of integrating functional MR imaging with radiation therapy treatment by using fiducial gold markers. Radiology 236(1), 311–317 (2005)
8. Klein, S., van der Heide, U.A., Lips, I.M., van Vulpen, M., Staring, M., Pluim, J.P.W.: Automatic segmentation of the prostate in 3D MR images by atlas matching using localized mutual information. Medical Physics 35(4), 1407–1417 (2008)
9. Kovar, D.A., Lewis, M., Karczmar, G.S.: A new method for imaging perfusion and contrast extraction fraction: input functions derived from reference tissues. J. Magn. Reson. Imaging 8(5), 1126–1134 (1998)
10. Li, Q., Sone, S., Doi, K.: Selective enhancement filters for nodules, vessels, and airway walls in two- and three-dimensional CT scans. Medical Physics 30(8), 2040–2051 (2003)
11. Roobol, M.J., Steyerberg, E.W., Kranse, R., Wolters, T., van den Bergh, R.C.N., Bangma, C.H., Schröder, F.H.: A risk-based strategy improves prostate-specific antigen-driven detection of prostate cancer. Eur. Urol. 57(1), 79–85 (2010)
12. Schröder, F.H., Hugosson, J., Roobol, M.J., Tammela, T.L.J., Ciatto, S., Nelen, V., Kwiatkowski, M., Lujan, M., Lilja, H., Zappa, M., Denis, L.J., Recker, F., Berenguer, A., Mttnen, L., Bangma, C.H., Aus, G., Villers, A., Rebillard, X., van der Kwast, T., Blijenberg, B.G., Moss, S.M., de Koning, H.J., Auvinen, A., E. R. S. P. C. Investigators: Screening and prostate-cancer mortality in a randomized european study. N. Engl. J. Med. 360(13), 1320–1328 (2009)
13. Stoutjesdijk, M.J., Veltman, J., Huisman, H., Karssemeijer, N., Barentsz, J.O., Blickman, J.G., Boetes, C.: Automated analysis of contrast enhancement in breast MRI lesions using mean shift clustering for ROI selection. Journal of Magnetic Resonance Imaging 26(3), 606–614 (2007)
14. Tanimoto, A., Nakashima, J., Kohno, H., Shinmoto, H., Kuribayashi, S.: Prostate cancer screening: the clinical value of diffusion-weighted imaging and dynamic MR imaging in combination with T2-weighted imaging. J. Magn. Reson. Imaging. 25(1), 146–152 (2007)
15. Tofts, P.S., Brix, G., Buckley, D.L., Evelhoch, J.L., Henderson, E., Knopp, M.V., Larsson, H.B., Lee, T.Y., Mayr, N.A., Parker, G.J., Port, R.E., Taylor, J., Weisskoff, R.M.: Estimating kinetic parameters from dynamic contrast-enhanced T(1)-weighted MRI of a diffusable tracer: standardized quantities and symbols. J. Magn. Reson. Imaging 10(3), 223–232 (1999)
16. Vos, P.C., Hambrock, T., Barenstz, J.O., Huisman, H.J.: Automated calibration for computerized analysis of prostate lesions using pharmacokinetic magnetic resonance images. In: Yang, G.-Z., Hawkes, D., Rueckert, D., Noble, A., Taylor, C. (eds.) MICCAI 2009. LNCS, vol. 5762, pp. 836–843. Springer, Heidelberg (2009)
17. Vos, P.C., Hambrock, T., Barenstz, J.O., Huisman, H.J.: Computer-assisted analysis of peripheral zone prostate lesions using T2-weighted and dynamic contrast enhanced T1-weighted MRI. Physics in Medicine and Biology 55(6), 1719–1734 (2010)

18. Vos, P.C., Hambrock, T., Hulsbergen van de Kaa, C.A., Fütterer, J.J., Barentsz, J.O., Huisman, H.J.: Computerized analysis of prostate lesions in the peripheral zone using dynamic contrast enhanced MRI. Medical Physics 35(3), 888–899 (2008)
19. Vos, P.C., Hambrock, T., Barentsz, J., Huisman, H.J.: Computer-aided detection of prostate lesions at diffusion-weighted mr using a dedicated hessian matrix-based detection scheme. In: Annual Meeting of the Radiological Society of North America (2009)
20. Wolf, A.M.D., Wender, R.C., Etzioni, R.B., Thompson, I.M., D'Amico, A.V., Volk, R.J., Brooks, D.D., Dash, C., Guessous, I., Andrews, K., DeSantis, C., Smith, R.A., American Cancer Society Prostate Cancer Advisory Committee: American cancer society guideline for the early detection of prostate cancer: update 2010. CA Cancer J. Clin. 60(2), 70–98 (2010)